



**HAL**  
open science

# HILS-based Demonstrator for Real-time Validation of Robust Control Strategies: An Electric Vehicle Application Case

Iulian Munteanu, Antoneta Iuliana Bratcu

► **To cite this version:**

Iulian Munteanu, Antoneta Iuliana Bratcu. HILS-based Demonstrator for Real-time Validation of Robust Control Strategies: An Electric Vehicle Application Case. IFAC WC 2023 - 22nd IFAC World Congress, IFAC, Jul 2023, Yokohama, Japan. hal-04062809

**HAL Id: hal-04062809**

**<https://hal.science/hal-04062809>**

Submitted on 7 Apr 2023

**HAL** is a multi-disciplinary open access archive for the deposit and dissemination of scientific research documents, whether they are published or not. The documents may come from teaching and research institutions in France or abroad, or from public or private research centers.

L'archive ouverte pluridisciplinaire **HAL**, est destinée au dépôt et à la diffusion de documents scientifiques de niveau recherche, publiés ou non, émanant des établissements d'enseignement et de recherche français ou étrangers, des laboratoires publics ou privés.

# HILS-based Demonstrator for Real-time Validation of Robust Control Strategies: An Electric Vehicle Application Case <sup>\*</sup>

Iulian MUNTEANU <sup>\*</sup> Antoneta Iuliana BRATCU <sup>\*</sup>

<sup>\*</sup> Univ. Grenoble Alpes, CNRS, Grenoble INP, GIPSA-lab  
38000 Grenoble, France (e-mails: iulian.munteanu,  
antoneta.bratcu@gipsa-lab.grenoble-inp.fr).

---

**Abstract:** This paper presents a demonstrator featuring closed-loop coupling of a robust-control-designed Power Management System (PMS) with a simulator – in the form of a mathematical model – of a multiple-storage-based microgrid, playing the role of the plant. The PMS ensures a reliability-aware coordinated control of the different energy storages, of various technologies, supplying a typically irregular load. Some usual applications are in stationary or mobile microgrids, like power supply systems on board of electric vehicles, the latter being the use case exemplified here. Being designed upon the hardware-in-the loop simulation (HILS) principle, the demonstrator allows calibration and real-time validation of the robust PMS and its pertinent closed-loop real-time tests in laboratory conditions. The rapid prototyping system dSPACE<sup>TM</sup> MicroAutoBox II is employed for embedding the microgrid model, whereas the robust PMS is embedded on a TI C2000 microcontroller unit. General design requirements and architecture of the demonstrator are detailed, then its customization to the considered application case is presented. Finally, a set of illustrative real-time tests – obtained by using a standard driving cycle – are presented and discussed.

*Keywords:* real time simulation and dispatching of power and energy systems, embedded computer control systems and applications, robust controller synthesis, application of power electronics.

---

## 1. INTRODUCTION

*In situ* preliminary experimental validation of control laws may be difficult because of unpredictability of operating conditions and associated risks and/or expensive costs. The *hardware-in-the-loop simulation* (HILS) principle is nowadays widely employed for rapid prototyping, its effectiveness being fully recognized. In this way, replicable experiments can repetitively be carried out in laboratory conditions on dedicated test rigs.

Generally speaking, the HILS concept consists in the closed-loop connection of both physical and software parts, in order to replicate in laboratory (controlled, customizable and safe) conditions the dynamic behaviour of an industrial process or system. The software part results from modelling those parts of the real system which will be *simulated* in real time – because it is too expensive and/or dangerous to use the *real* parts – whereas the physical part is taken as it is from that system.

Since its definition and introduction at the beginning of the 1990s for developing and testing control structures for mechanical equipments (Hanselmann (1993)) – HILS applications in the automotive industry using the MATLAB /Simulink software on a dSPACE<sup>TM</sup> platform date back to 1996 (Hanselmann (1996), Kiffmeier (1996))

– HILS concept has increasingly been used – in particular, for control law rapid prototyping – being now involved in other modern concepts such as, for example, the digital twin. The main idea is to embed a control law on a numerical device (hardware under test – HUT), which is further connected in closed loop to a computing unit that runs a real-time mathematical model of the plant. This device is typically a microcontroller unit (MCU) and can be used in conjunction with other architectures, *e.g.*, an FPGA (Prochazka *et al.* (2021)).

## 2. ARCHITECTURE OF THE HILS-BASED DEMONSTRATOR

The HILS-based demonstrator architecture results according to a predefined set of requirements, some of which are general for the real-time control applications design and some other ones are specific for the considered application.

*General requirements.* A HILS setup must provide representative, controllable and reproducible conditions for test and validation of various control strategies. Thus, it should have real-time capabilities, enabled by fast-computation processing units and accompanied by automatic code generation for an as large as possible real-time targets, namely state-of-the-art MCUs, widely used in industry. Generic flexibility features must rely upon portable hardware and evolutive software architecture, such that new components or updates to be easily added. Not least, an user-friendly interface, with extensive capabilities, is necessary.

---

<sup>\*</sup> This work was funded between 2017 and 2018 by Institut Carnot *Logiciels et Systèmes Intelligents* (LSI), in the framework of technology pre-transfer funding scheme.

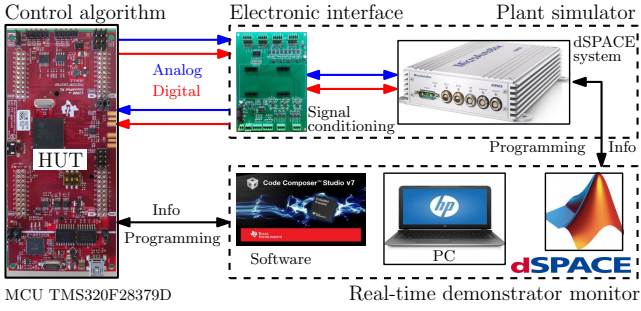


Fig. 1. General configuration of the demonstrator.

**Hardware configuration.** Fig. 1 shows the real-time closed loop composed of a coupling between the plant simulator and the MCU board hosting the control algorithm. Here, a Texas Instruments (TI) C2000 Delfino MCU, mounted on a LAUNCHXL-F28379D board, is chosen to embed the control (\*\*TI MCU (2017a)), while the plant is real-time simulated by using a dSPACE<sup>TM</sup> MicroAutoBox II platform, with DS1513 I/O board (\*\*dSPACE (2017a)). The two devices exchange analog and digital signals *via* a dedicated I/O electronic signal interface. The entire demonstrator is monitored by a PC HP Zbook 15 G3 mobile workstation, which also hosts the real-time programming for both targets, MCU and dSPACE<sup>TM</sup> MicroAutoBox II.

Fig. 2 shows a photo of the assembled demonstrator, which has been designed such that its components are impaled one into another, at the lowermost level being the dSPACE<sup>TM</sup> system (noted by "1" in the figure) and on the top the LaunchPad board with the TI C2000 MCU (noted by "4"). The electronic interface, "3", and the connection break-out box, "2", are placed in the middle.

**Software elements.** Software components are belonging to three groups: software running off-line on PC workstation; codes running in real-time on either targets: TI C2000 MCU and dSPACE<sup>TM</sup> MicroAutoBox II; real-time operation monitoring software running on PC workstation.

The first category includes the PC operating system as support for all programming software, and MCU specific drivers, *e.g.*, those of communication protocol conversion.

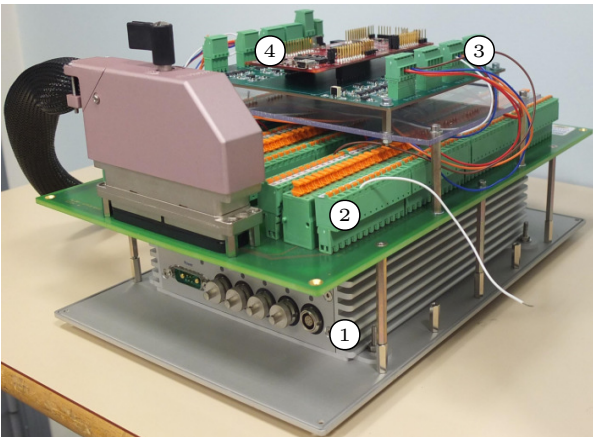


Fig. 2. Demonstrator's hardware configuration (photo).

As the controller design relies upon a model-based approach, implemented under MATLAB /Simulink software environment (\*\*MathWorks (2022)), some specialized

toolboxes are used to design and build controller and plant simulator diagrams – among them, toolboxes enabling real-time operation and also MCU-dedicated software packages, like "Embedded Coder Support Package for TI C2000 Processors". The latter one is used in conjunction with Code Composer Studio (CCS) Integrated Development Environment (IDE) (\*\*TI CCS (2017b)) and ControlSUITE<sup>TM</sup> (\*\*TI CS (2017c)) for TI C2000 MCU code generation. In addition to these, Real-Time Interface (RTI) is used to extend the C code generator Simulink Coder<sup>TM</sup> for automatic implementation of Simulink models on the real-time hardware. Here, it is used to convert plant simulator diagram into dSPACE<sup>TM</sup> MicroAutoBox II target code.

The second class of software is composed of the real-time codes built by using the above-mentioned tools, while the third class is based on ControlDesk universal experiment software (\*\*dSPACE (2017b)), used to monitor MicroAutoBox II operation.

### 3. APPLICATION CASE: ROBUST PMS FOR EV ON-BOARD MULTI-STORAGE POWER SUPPLY SYSTEM

A multi-storage power supply system on board of an electric vehicle (EV) is here considered, which illustrates hybridization of a number of technologically-different electrical power sources. Hybridization is a state-of-the-art solution widely used for covering non-uniform (even erratic) power availability/demand in a wide area of applications. Combining two or more electrical power sources, each of which is specialized in a certain dynamic range, represents an optimal techno-economical solution (Miller *et al.* (2009)). In EV applications, fuel cells or electrochemical batteries are used for supplying the slow, low-frequency variations of power demand – according to Ragone's taxonomy (Florescu *et al.* (2012)), these are *high-energy-density* sources – while ultracapacitors or flywheels are widely used for either providing or absorbing the rapid, high-frequency variations of power demand – these are *high-power-density* sources. Also, renewable energy systems (*e.g.*, PV panels) may be inserted into power system for reducing fuel consumption and increasing vehicle autonomy. Effective coordination of these complementary sources is ensured by means of a Power Management System (PMS).

To fix ideas, a three-storage EV power supply configuration as in Fig. 3 is considered next, where a fuel cell, a battery and an ultracapacitor are connected on a common DC link, which supplies the main EV electrical motor (Nwesaty *et al.* (2016)). Each storage is current-controlled by means of a DC-DC power electronics synchronous buck converter. References to be provided to low-level PI-based current tracking loops, are denoted by  $\langle \cdot \rangle$  in Fig. 3. The hybridization comes here from the need to protect the fuel cell from the sudden power load variations that risk to negatively affect its reliability and lifetime. Instead, such variations may easier be dealt with by inserting an ultracapacitor system in parallel on the DC link, to be able to provide large amount of electrical power in a short time. A drawback is that the ultracapacitor will be empty/full in short time, because of its limited capacity. Thus, the battery adds flexibility by supplying/drawing not only

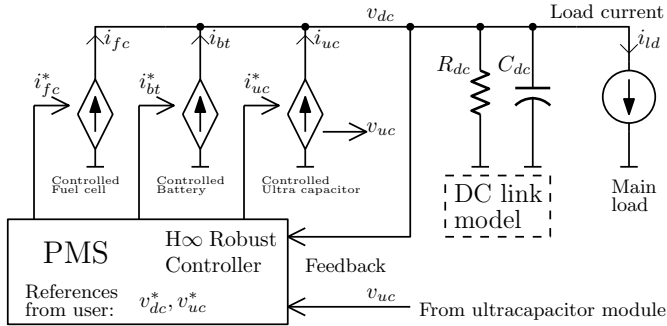


Fig. 3. Configuration of the EV power supply system.

a part of low-frequency current, but also the medium-frequency current component.

The particularity of having three different storages in a power supply on board of EVs has been considered sufficiently generic and illustrative for various management methods proposed in the literature (*e.g.*, Thounthonga *et al.* (2009), Zandi *et al.* (2011)).

For this system a threefold control objective is stated. Thus, the primary control target is to maintain DC-link voltage at some imposed setpoint,  $v_{dc}^*$ , irrespective of the current load. The main load is the EV AC motor (usually a permanent-magnet synchronous motor) driven by an inverter. The motor operates in generator regimes while vehicle is braking. The electrical current demanded/supplied by the inverter,  $i_{ld}$ , acts as an uncontrollable current source (disturbance). Second, current references to each storage must be provided in their specific operating dynamic domain, thus optimizing their operation and reducing sizing/design task complexity; reliability-aware aspects are thus accounted for in the control design. Finally, ultracapacitor voltage must be loosely maintained around some imposed value,  $v_{uc}^*$  – *e.g.*, about 70% of rated – to avoid operating limits of ultracapacitor under-/over-voltage.

The above-listed control objectives have been cast as a robust disturbance-rejection problem, solved by designing an  $\mathcal{H}_\infty$ -based PMS. Thus, the control effort is split between the sources by using our approach in Nwesaty *et al.* (2015, 2016), which casts the desired frequency domains of sources into spectral-shaped sensitivity functions. The PMS shown in Fig. 3 has  $v_{dc}$  and  $v_{uc}$  errors as inputs, while its outputs are current references of fuel cell,  $i_{fc}^*$ , battery,  $i_{bt}^*$ , and ultracapacitor,  $i_{uc}^*$ , cast in low-, medium- and high-frequency domains, respectively.

Unlike more classical solutions, such as, *e.g.*, the one based on filtering (Florescu *et al.* (2012)), this MIMO  $\mathcal{H}_\infty$  approach provides additional degrees of freedom in design, such that to be able to perform multi-criteria optimization in the sense of robustifying closed-loop performance in relation to the operating point and parameter uncertainties. The design procedure has been coded in MATLAB and outputs a single controller as a dynamic system, in a form ready to be automatically translated in executable code for the chosen target MCU.

Flexibility is paid by controller complexity. However, it was proved that embedding the PMS for the considered use case has only required a small amount of the TI C2000 MCU computing resources, as specified further in Section 5. On the other hand, the non structured pattern of the  $\mathcal{H}_\infty$  controller renders it relatively difficult to debug

and requires extensive attention when embedding different additional conditioning, *e.g.*, anti-windup loops.

#### 4. CUSTOMIZATION OF THE DEMONSTRATOR FOR THE EV ON-BOARD ROBUST PMS VALIDATION

Adjustments have been made to the basic demonstrator configuration (see Fig. 1), in order to customize it for the considered application case. Thus, both hardware and software elements have been added, the latter in relation to codes developed on both MicroAutoBox II and TI C2000 MCU, such as user interfaces implemented in ControlDesk and TI C2000 Simulink console.

*ControlDesk interface.* An user-friendly and intuitive user interface has been built in ControlDesk, having in its center a diagram representing the EV’s three-storage power supply system (see Fig. 4); this allows supervision of the closed-loop operation and user control of simulation scenarios *via* digital signals.

The user-input zone (at the left side of the figure) has been enriched with more driving cycle selection possibilities (up to nine), cycle gain, possibility of configuring  $v_{dc}$  measurement noise (by means of its base frequency and standard deviation). LEDs concerning controller activation, storage systems status, pushbuttons for powering, enabling and configuring subsystems are included. A manual slider is present to allow configuring a desired current level; it is limited at  $\pm 60$  A as in steady-state the fuel cell is not able to provide enough current such that to overcome atypically large loads. A time counter for supervising load cycles has been added at the top-left corner of the screen.

*TI C2000 MCU console.* The Simulink console, supervising TI C2000 MCU operation *via* serial peripheral interface, see Fig. 5, has been upgraded with new capabilities, including FFTs of sources’ currents. This console allows switching between the two types of PMS – the robust one and the PI-based one – by toggle the “Ctrl Mode” button (at the left side) and features displays of system states, control errors and outputs of the controller. It also allows real-time computing and visualization of the three sources’ currents spectra.

*Joystick.* An analog joystick has been developed in order to facilitate input of load current in an arbitrary mode by an user. Its operation is configured *via* the ControlDesk interface; the user can select current load source either from the manual slider or from joystick.

A global picture of the demonstrator can be seen in Fig. 6.

#### 5. CLOSED-LOOP REAL-TIME VALIDATION RESULTS

Effective operation of the demonstrator supposes two major steps. First, one prepares the two Simulink diagrams for both the plant simulator and the PMS controller and associated MATLAB files. Then, these diagrams are compiled and the resulted code is uploaded to the specific targets. The two user interfaces are separately built using dedicated mechanisms in Simulink and ControlDesk.

In a second phase, demonstrator can be used for either validation of the  $\mathcal{H}_\infty$ -based PMS control law, or for system closed-loop capabilities demonstration. Once the operation

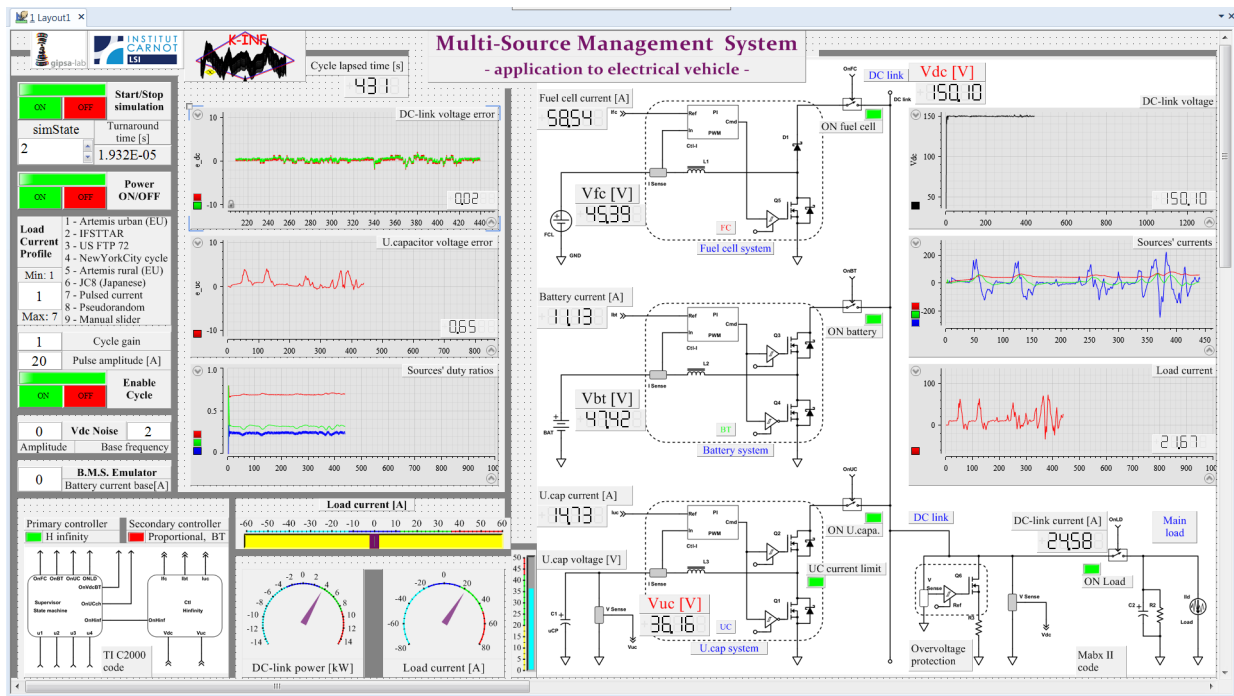


Fig. 4. ControlDesk interface with customized capabilities, allowing plant supervision.

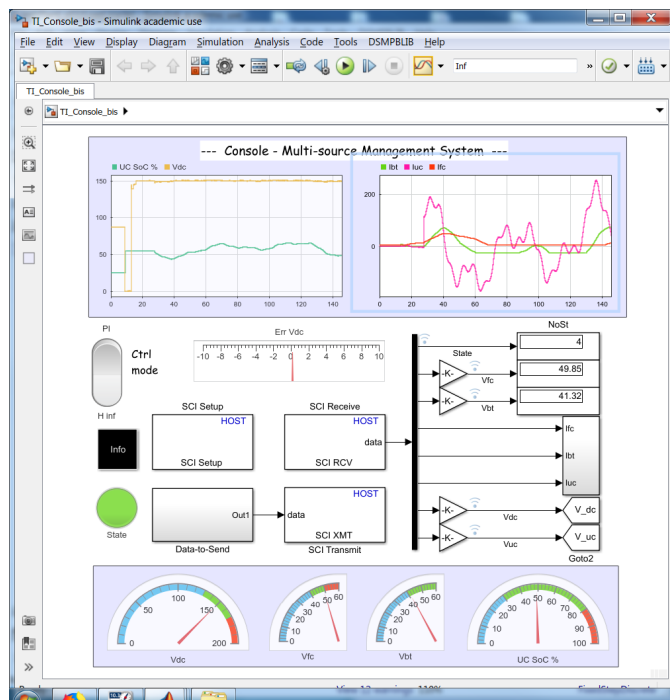


Fig. 5. Simulink console for TI C2000 MCU embedding the robust PMS.

goal having been defined, one chooses the most pertinent scenario to apply, allowing time- and frequency-domain analysis of closed-loop system behaviour in real time.

*Performance of the embedded robust PMS code.* TMS 320F28379D MCU has been used for effective control code embedding; its computing performance is given by 800 MIPS at 200 MHz and 204 kB RAM. A thorough analysis of its usage in terms of both computational burden and memory allocation has been done. This allows assessing

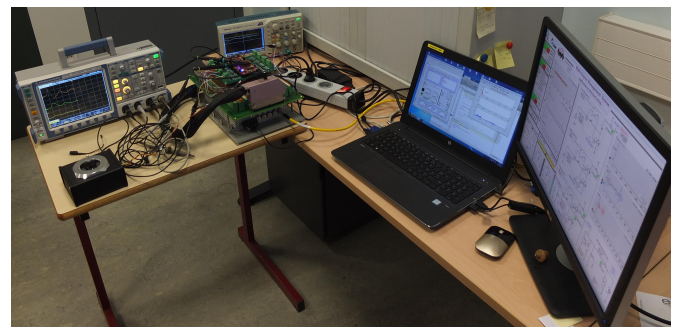


Fig. 6. Global view of the real-time validation setup build around the HILS-based demonstrator – photo at GIPSA-lab.

either a downgrade to a less expensive and less powerful MCU, or the reserve in terms of computational power and memory that could be used if embedding of a more complex control would be aimed at. The allocated memory was estimated from information given by the linking process: the total memory is about 20 kB, *i.e.*, about 10% of the MCU available memory.

As regards the processing power reserve evaluation, the computational time of controller's critical actions is about 25.3  $\mu$ s out of the 100  $\mu$ s available (corresponding to the sampling frequency of 10 kHz), so the interrupt takes roughly 25% of the total available computational time.

Hence, a large amount of code can still be executed by the chosen MCU within the chosen sampling time, so further complexifying of the control law is totally affordable. Moreover, note also that it is in this case about a dual-processor architecture, so only half of computing power is actually used (400 MIPS). The other way round, if the control law does not need to be further enhanced, then a less expensive MCU, *e.g.*, in the Delfino<sup>TM</sup> class, can be envisaged for further development, *e.g.*, TMS320F2833x (with 100-150 MIPS and 68 KB RAM).

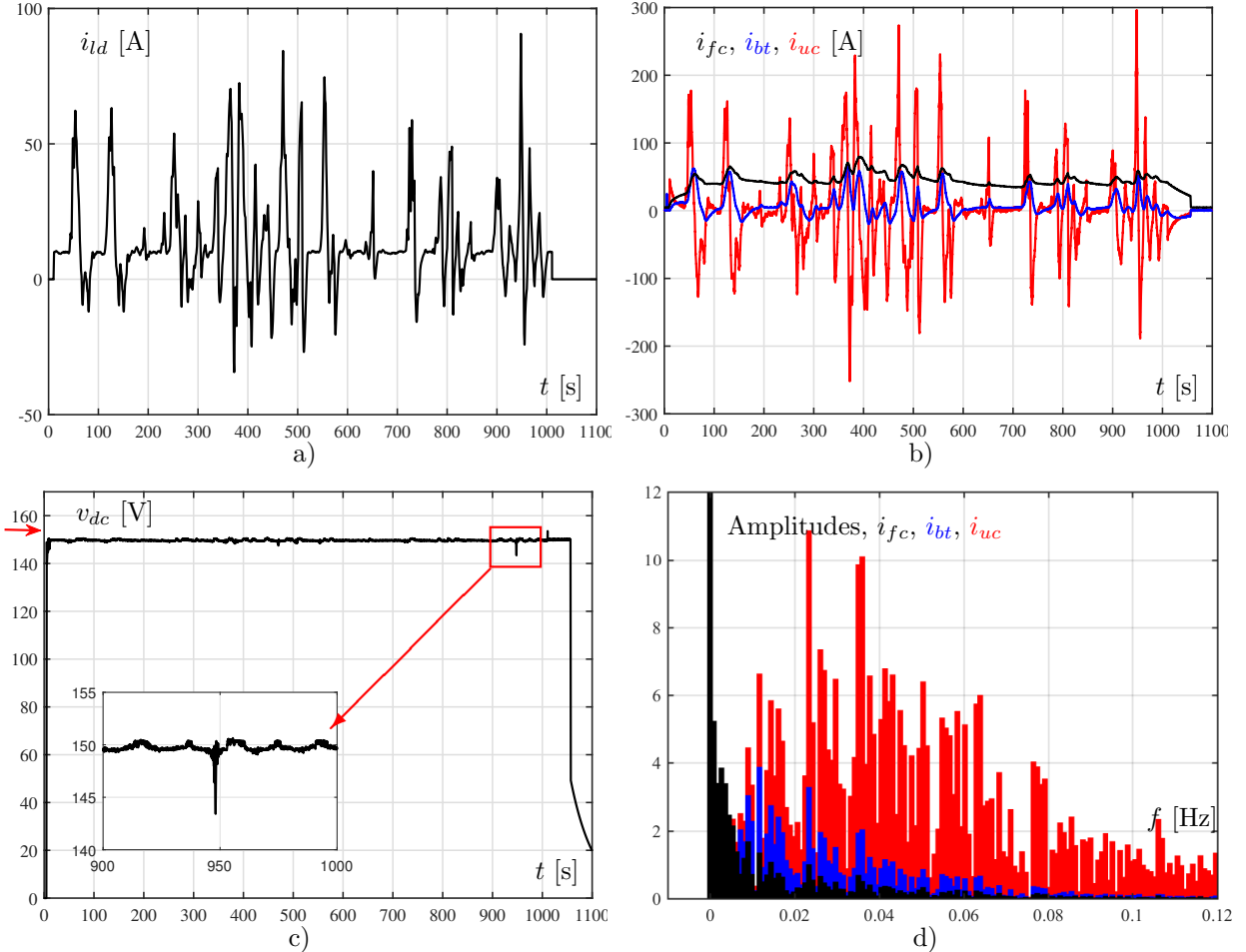


Fig. 7. Closed-loop PMS validation in response to “Artemis Urban” driving cycle (\*\*\*) (2023): a) load current; b) sources’ currents (black line – fuel cell, blue line – battery, red line – ultracapacitor); c) DC-link voltage; d) spectral characteristics of sources’ currents: black bars – fuel cell, blue bars – battery, red bars – ultracapacitor.

*Real-time closed-loop results under “Artemis Urban” driving cycle.* The European “Artemis Urban” driving cycle has been chosen to illustrate closed-loop effectiveness of the designed PMS on board of a three-storage EV, whose main parameters are listed in the Appendix A. Time evolutions presented next have been obtained by means of the ControlDesk interface in Fig. 4. Fig. 7a) contains the corresponding current load profile,  $i_{ld}$ .

Fig. 7c) shows a very fast regulation of DC-link voltage around its setpoint value ( $v_{dc}^* = 150$  V), with a maximum error of about 2.5%. Fig. 7b) illustrates that the dynamic separation of sources’ currents is effective: fuel cell current (black line) contains only low frequencies, while ultracapacitor current (red line) contains zero-average high-frequency components. The battery supplies medium frequencies (blue line). So, the high-power-density storage effectively protects the other two, high-energy-density ones. The same idea is illustrated in Fig. 8a), where oscilloscope captures zoomed on the first 400 s are shown, with the associated controlled voltages in Fig. 8b).

Corresponding FFT spectra of each of the sources’ currents in response to the load current are presented in Fig. 7d), thus equivalently illustrating sources’ dynamic separation in the frequency domain: ultracapacitor current (red bars) is spread towards high frequencies, while fuel cell

current (black bars) occupies the low frequencies – with a very large DC component – with battery current spectrum (blue bars) being placed in the mid-frequency range.

## 6. CONCLUSION

This paper has dealt with the systematic design, building and performance assessment of a HILS-based demonstrator dedicated to rapid prototyping and preliminary control law validation in laboratory – *i.e.*, safe, controllable and reproducible – conditions. The case of a three-storage power supply system on board of an electric vehicle, managed by a robust,  $\mathcal{H}_\infty$ -based power management system, has been chosen as application and its proof of concept has been thoroughly performed. Choice of the  $\mathcal{H}_\infty$  approach has been justified by the necessity of robustifying the closed-loop performance in relation to the operating point and parameter uncertainties. The rapid prototyping system dSPACE<sup>TM</sup> MicroAutoBox II has been employed for embedding the power supply system model, with the robust,  $\mathcal{H}_\infty$ -based PMS being embedded on a Texas Instruments general-purpose microcontroller unit.

Starting from a generic set of requirements, focus has been put on the flexibility of the demonstrator basic structure, which allows customizing and upgrading it for a particular application. Not least, it has been shown that embedding

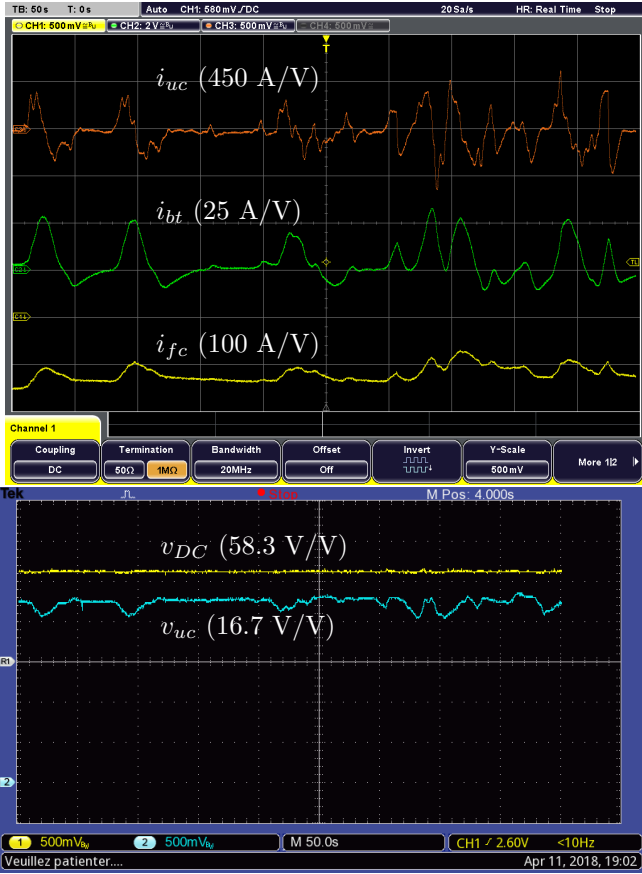


Fig. 8. Zoomed oscilloscope captures for “Artemis Urban” cycle: a) sources’ currents; b) controlled voltages.

of quite complex controls (such as a robust one) is perfectly affordable from a cost–performance trade-off viewpoint.

#### ACKNOWLEDGEMENTS

The authors are grateful to Julien MINET, Sophie MINICAULT and Rémy JACCAZ, who helped with electronic interface and mechanical design.

#### REFERENCES

- \*\*\*dSPACE (2017a). dSPACE™ MicroAutoBox II. Available: <https://www.dspace.com/en/pub/home/products/hw/micautob.cfm>.
- \*\*\*dSPACE (2017b). ControlDesk universal experiment software. Available: <https://www.dspace.com/en/pub/home/products/sw/experimentandvisualization/controldesk.cfm>.
- \*\*\*Texas Instruments (2017a). C2000 Delfino MCUs F28379D LaunchPad Development Kit. Available: <http://www.ti.com/tool/launchxl-f28379d>.
- \*\*\*Texas Instruments (2017b). Code Composer Studio (CCS) Integrated Development Environment (IDE). Available: [http://www.ti.com/tool/ccstudio?DCMP=dsp\\_ccs\\_v4&HQS=ccs](http://www.ti.com/tool/ccstudio?DCMP=dsp_ccs_v4&HQS=ccs).
- \*\*\*Texas Instruments (2017c). ControlSUITE™ software suite. Available: <http://www.ti.com/tool/controlsuite>.
- \*\*\*Model-Based Design Approach (2022). Available: <https://fr.mathworks.com/solutions/model-based-design.html>.
- \*\*\*“Artemis Urban” driving cycle (2023). Available: <https://dieselnet.com/standards/cycles/artemis.php>.
- A. Florescu, S. Bacha, I. Munteanu, and A.I. Bratcu (2012). Frequency-separation-based energy management control strategy of power flows within electric vehicles using ultracapacitors. In: *IECON 2012-38th Annual Conference on IEEE Industrial Electronics Society*, pages 2957–2964.
- H. Hanselmann (1993). Hardware-in-the loop simulation as a standard approach for development, customization, and production test of ECUs. In: *Procs. of International Pacific Conference On Automotive Engineering*, SAE Technical Paper 931953.
- H. Hanselmann (1996). Hardware-in-the-loop simulation testing and its integration into a CACSD toolset. In: *Procs. of the Joint Conference on Control Applications Intelligent Control and Computer Aided Control System Design*, Dearborn, MI, U.S.A., September 1996, pages 152–156.
- U. Kiffmeier (1996). A hardware-in-the-loop testbench for ABS controllers. In: *Procs. of the 1st International Conference on Control and Diagnostics in Automotive Applications*, Genova, Italy, October 1996.
- J.M. Miller, T. Bohm, T.J. Dougherty, and U. Deshpande (2009). Why hybridization of energy storage is essential for future hybrid, plug-in and battery electric vehicles. In: *IEEE Energy Conversion Congress and Exposition*, 2009, San Jose, CA, U.S.A., pages 2614–2620.
- W. Nwesaty, A.I. Bratcu, and O. Sename (2015). Reduced-order LPV controller for coordination of power sources within multi-source energy systems. *IFAC-PapersOnLine*, vol. 48, no. 14, pages 132–137.
- W. Nwesaty, A.I. Bratcu, and O. Sename (2016). Power sources coordination through multivariable LPV/Hinf control with application to multi-source electric vehicles. *IET Control Theory and Applications*, vol. 10, no. 16, pages 2049–2059.
- F. Prochazka, S. Krüger, G. Stomberg, and M. Bauer (2021). Development of a hardware-in-the-loop demonstrator for the validation of fault-tolerant control methods for a hybrid UAV. *CEAS Aeronautical Journal*, vol. 12, pages 549–558.
- P. Thounthonga, S. Raël, and B. Davat (2009). Energy management of fuel cell/battery/supercapacitor hybrid power source for vehicle applications. *Journal of Power Sources*, vol.193, pages 376–385.
- M. Zandi, A. Payman, J.-P. Martin, S. Pierfederici, B. Davat, and F. Meibody-Tabar (2011). Energy Management of a Fuel Cell/Supercapacitor/Battery Power Source for Electric Vehicular Applications. *IEEE Transactions on Vehicular Technology*, vol. 60, no. 2, pages 433–443.

#### Appendix A. EV POWER SUPPLY MAIN PARAMETERS

- rated power:  $P_{dc} = 15$  kW;
- DC link: voltage  $v_{dc}^* = 150$  V, capacity  $C_{dc} = 10000$   $\mu F$ ;
- fuel cell rated voltage  $E_{0f} = 50$  V;
- lead-acid battery: voltage 48 V, capacity 12.6 Ah;
- ultracapacitor: capacity  $C_0 = 2600$  F, maximum voltage 42 V, minimum voltage 32 V;
- current tracking loops’ time constant  $T_C = 2$  ms.